energies

MDPI

Article

Construction of Chemically Crosslinked Sulfonated Poly(aryl ether ketone) Networks for Polymer Electrolyte Membranes

Zhenchao Liu [1], Bing Liang [1], Zizhen Xie [1], Wei Hu [2] and Baijun Liu [1,*]

[1] College of Chemistry, Jilin University, 2699 Qianjin Street, Changchun 130012, China; zcliu@ciac.ac.cn (Z.L.)
[2] School of Chemistry, Northeast Normal University, 5268 Renmin Street, Changchun 130024, China; huw884@nenu.edu.cn
* Correspondence: liubj@jlu.edu.cn

Abstract

Polymer electrolyte membranes serving in proton exchange membrane fuel cells (PEMFCs) and direct methanol fuel cells (DMFCs) must possess sufficient mechanical–dimensional stability and excellent proton conducting capacity. Derived from the successful syntheses of two different sulfonated poly(aryl ether ketone)s bearing functional amine groups, two series of novel epoxy-crosslinked and silane-crosslinked sulfonated poly(aryl ether ketone) electrolyte networks are constructed for highly conductive and mechanically stable proton exchange membranes. The designed multi-component architecture, which integrates a moderate-ion-exchange-capacity sulfonated poly(aryl ether ketone) (moderate-IEC SPAEK), a high-IEC SPAEK, and a tailored crosslinker (epoxy or silane), enables a breakthrough in decoupling the traditional trade-off between conductivity and stability. The resulting membranes exhibit an outstanding combination of properties: exceptional proton conductivity exceeding 0.18 S cm^{-1} at 100 °C, tensile strength above 28.80 MPa, and enhanced chemical resistance, thermo-oxidative stability, and competitive direct methanol fuel cell performance. This work establishes a rational design strategy for crosslinked multi-component membranes as a promising platform for next-generation high-performance fuel cells.

Keywords: polymer electrolyte membranes; sulfonated poly(aryl ether ketone)s; crosslinked networks; high conductivity

1. Introduction

Fuel cells have emerged as pivotal energy conversion devices, renowned for their high energy conversion efficiency and ability to transform the chemical energy of fuels into electricity with minimal greenhouse gas emissions [1–3]. Among the diverse array of fuel cell technologies, proton exchange membrane fuel cells (PEMFCs) and direct methanol fuel cells (DMFCs) have attracted significant interest due to their capacity to deliver high power density at relatively low operating temperatures [4,5]. Central to the performance of PEMFCs and DMFCs are polymer electrolyte membranes (PEMs), which must simultaneously facilitate efficient proton transport from anode to cathode and act as an effective barrier against fuel crossover, all while maintaining robust mechanical and dimensional stability under operating conditions [6–8]. To date, perfluorosulfonic acid membranes, most notably DuPont's Nafion®, have dominated the commercial landscape owing to their exceptional chemical stability and high proton conductivity [9,10]. However, their widespread

Academic Editors: Antonino S. Aricò and Francesco Lufrano

Received: 6 April 2026
Revised: 21 May 2026
Accepted: 5 June 2026
Published: 11 June 2026

adoption is constrained by inherent limitations, including high manufacturing costs and excessive fuel permeability, which have spurred extensive research into alternative membrane materials [11,12].

Sulfonated aromatic polymers, such as sulfonated poly(aryl ether ketone)s (SPAEKs), sulfonated polysulfones, sulfonated polyimides, and sulfonated polybenzimidazoles, have been extensively investigated as promising candidates to replace perfluorinated membranes [13,14]. Among these, SPAEKs are particularly noteworthy due to the inherent thermal and mechanical robustness of the poly(aryl ether ketone) (PAEK) backbone, which can be functionalized with sulfonic acid groups via direct sulfonation or through the polymerization of sulfonated monomers [15–17]. Compared to Nafion®, SPAEK-based membranes offer advantages including simplified synthesis, lower cost, and reduced fuel crossover. Nevertheless, a fundamental trade-off persists in nearly all hydrocarbon-based PEMs: achieving high proton conductivity necessitates a high ion exchange capacity (IEC), which in turn often leads to excessive water uptake, pronounced swelling, and consequent deterioration of mechanical properties under the hydrated, elevated-temperature conditions typical of fuel cell operation [18–20].

To overcome this limitation while pursuing conductivity comparable to Nafion®, diverse strategies have been explored, encompassing both the molecular design of SPAEKs and their physical or chemical modification. For instance, multi-block copolymers containing highly sulfonated segments and grafted SPAEKs with locally concentrated acid groups have been designed to induce well-defined hydrophilic–hydrophobic phase separation, thereby promoting the formation of interconnected proton conducting channels [21,22]. Although such structures can yield high conductivity, they frequently suffer from synthetic complexity and compromised mechanical integrity [23]. Alternatively, the incorporation of performance-enhancing fillers—such as inorganic nanoparticles (e.g., sulfonated POSS, SiO_2, zeolite) or organic polymers (e.g., PVA, cellulose, chitosan)—into SPAEK matrices has been widely studied [24,25]. However, these approaches often encounter drawbacks related to filler aggregation at higher loadings, which can impair membrane homogeneity, reduce proton mobility, and ultimately diminish overall performance [26–28]. For example, Du et al. observed that sulfonated SiO_2 nanoparticles aggregated at 10 wt% loading, leading to decreased water uptake and conductivity [29]. Similarly, Hou et al. reported that exceeding 5 wt% nanocellulose content in sulfonated poly(arylene ether ketone) composites resulted in reduced proton conductivity, likely due to obstructed proton pathways [30].

A critical consideration in the design of high-performance SPAEK-based PEMs is the precise control of the degree of sulfonation (DS), which directly governs the IEC and must be carefully balanced against chemical durability and dimensional stability [31]. In this context, chemical crosslinking has emerged as a highly effective strategy to mitigate excessive swelling while preserving—or even enhancing—proton conductivity. By forming covalent networks, crosslinking can restrict polymer chain mobility, improve mechanical strength, and promote the formation of more stable and interconnected hydrophilic domains conducive to proton transport [32,33]. Recent studies underscore that crosslinked SPAEK membranes exhibit not only superior dimensional and mechanical stability but also often demonstrate improved oxidative resistance and reduced methanol permeability, making them particularly suitable for DMFC applications [34,35].

Building on these insights and our previous work concerning crosslinked SPAEK systems [34,36], this study presents a systematic comparative investigation of two distinct crosslinking chemistries, namely epoxy-based and silane-based approaches, applied to a tailored pair of amino-functionalized SPAEKs possessing differentiated backbone ion exchange capacities. In this system, a moderate-IEC, fluorine-containing SPAEK (Am-6F-SPAEK) functions as the structural matrix, while a high-IEC SPAEK (Am-SPAEK-H) is

introduced as a conductivity-enhancing component, resulting in the formation of miscible blends. These blends are subsequently transformed into durable three-dimensional networks through reaction with either epoxy or silane crosslinkers.

The novelty of this work extends beyond the application of crosslinking as a known strategy. It is rooted in a systematic comparative investigation of two fundamentally distinct crosslinking mechanisms, namely epoxy-based and silane-based approaches, and their respective effects on the water uptake ratio, swelling ratio, mechanical properties, proton conduction, and methanol barrier performance of blend membranes with otherwise similar composition. This direct comparison offers unique insights into the structure–property relationships governing crosslinked SPAEK systems, an aspect that has received limited attention in prior studies focusing predominantly on a single crosslinking method. By clarifying the distinct roles of epoxy and silane crosslinks in microstructural organization and property modulation, this research aims to establish clearer design principles for developing next-generation high-performance polymer electrolyte membranes suitable for both proton exchange membrane fuel cell and direct methanol fuel cell applications.

2. Experimental

2.1. Materials

Phenylhydroquinone (97%, Sigma-Aldrich Co., LLC, St. Louis, MO, USA) and 4,4′-difluorobenzophenone (DFBP, Yianbian Chemical Factory, Yanbian, Jilin, China) were used as received without purification. Resorcinol diglycidyl ether (RDGE, 94%), 4,4′-(hexafluoroisopropylidene)diphenol (6FBPA, 98%) and 3-glycidyloxypropyltrimethoxysilane (GOPTS, 97%) were purchased from Shanghai Aladdin Bio-Chem Technology Co., Ltd., Shanghai, China. (4-Amino)phenylhydroquinone (4-AmPHQ) was synthesized in our lab through a two-step coupling–reduction reaction [34]. Sodium 5,5′-carbonylbis(2-fluorobenzene-sulfonate) (SDFBP) was prepared according to a procedure described by Wang et al. [35]. Potassium carbonate (K_2CO_3, 99%) was purchased from Sinopharm Chemical Reagent Co., Ltd., Beijing, China. All the other chemicals were obtained from commercial sources and purified by a conventional method.

2.2. Syntheses of the Sulfonated Polymers with a Designed Structure and IEC Value

2.2.1. Fluorinated SPAEK with Amino Groups

A fluorine-containing poly(aryl ether ketone) bearing sulfonic acid and amino groups (Am-6F-SPAEK) was synthesized through a copolymerization of two bisphenols and two difluoro-monomers (Scheme 1). A typical synthesis procedure of Am-6F-SPAEK is as follows: 0.4024 g (2 mmol) of 4-AmPHQ, 2.6898 g (8 mmol) of 6FBPA, 1.0910 g (5 mmol) DFBP, 2.1146 g (5 mmol) of SDFBP and 3.317 g (12 mmol) of K_2CO_3 were added into a three-necked flask with a Dean–Stark trap and a mechanical stirrer under nitrogen. DMSO (19 mL) and toluene (15 mL) were used as solvent and azeotropic reagent, respectively. The reaction mixture was refluxed at 120–130 °C for 3 h to remove the water in the reaction system. After dehydration and removal of toluene, the reaction temperature was increased to 160 °C and held at this temperature for another 6 h.

The resulting polymer fiber was received after pouring the vicious solution into deionized water. It was pulverized by a high-speed blender, washed with deionized water and ethanol several times to remove the salts and solvents, and dried at 80 °C in a vacuum oven for 24 h prior to use. Its inherent viscosity was 0.88 dL/g.

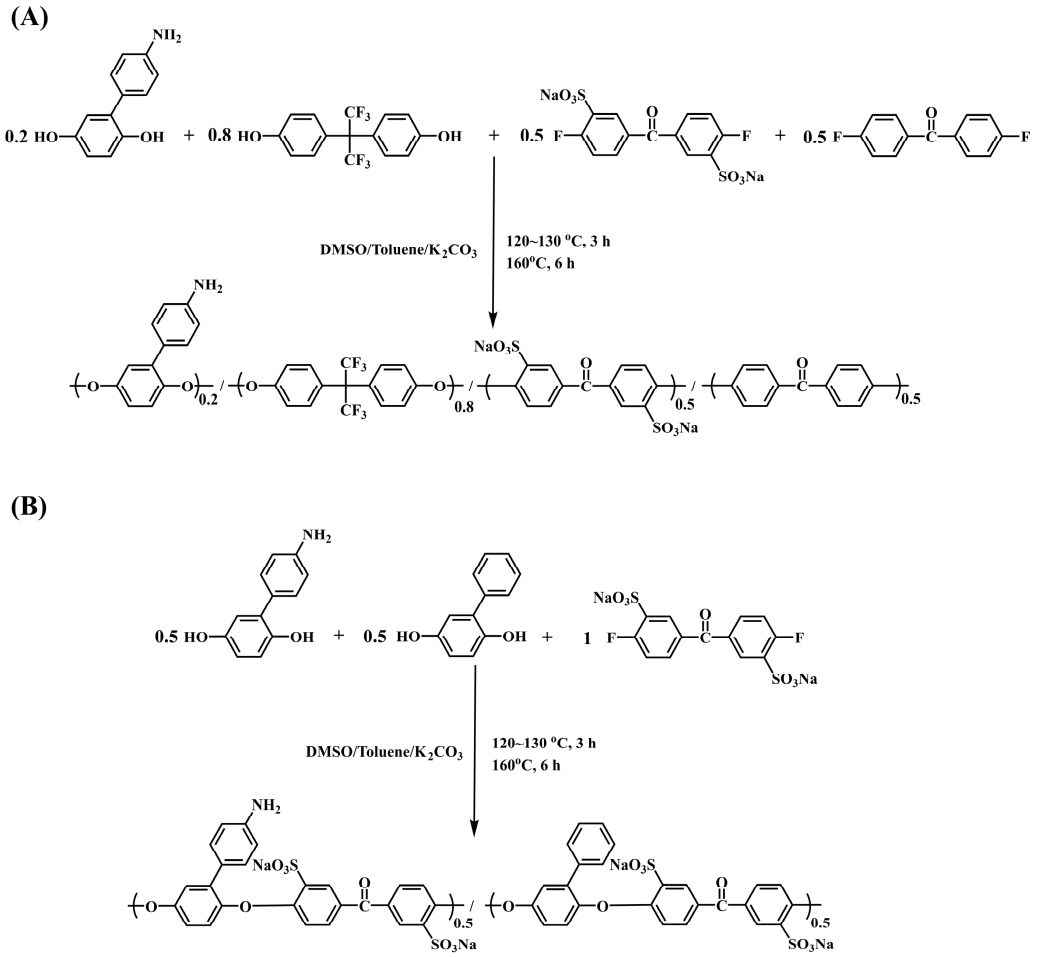

Scheme 1. Synthetic routes of Am-6F-SPAEK (**A**) and Am-SPAEK-H (**B**).

2.2.2. High-IEC SPAEK with Amino Groups

A high-IEC (high content of sulfonic acid groups) poly(aryl ether ketone) with sulfonic acid and amino groups (Am-SPAEK-H) was synthesized based on a bisphenol, an amino-functionalized bisphenol and a sulfonated difluoro-monomer. The synthesis procedure of Am-SPAEK-H is as follows: 1.0060 g (5 mmol) of 4-AmPHQ, 1.6811 g (5 mmol) of 6FBPA, 4.2292 g (10 mmol) of SDFBP and 3.318 g (12 mmol) of K_2CO_3 were added into a three-necked flask with a Dean–Stark trap and a mechanical stirrer under nitrogen. DMSO (18 mL) and toluene (15 mL) were used as solvent and azeotropic reagent, respectively. The reaction mixture was refluxed at 120–130 °C for 3 h to remove the water in the reaction system. After dehydration and the removal of toluene, the reaction temperature was increased to 140 °C and held at this temperature for another 6 h. The viscous polymer solution was slowly poured into excess ethanol to precipitate the crude product. The resulting solid was collected and then transferred into a dialysis bag with a molecular weight cutoff of 8000 Da. Dialysis was performed against deionized water for 48 h to remove residual water-soluble reactants, salts, and small-molecule byproducts. The water was renewed at regular intervals to facilitate the purification process. After dialysis, the purified polymer was collected and dried under vacuum. Its inherent viscosity was 0.17 dL/g and its theoretical IEC value was 3.75 mmol/g.

2.3. Preparation of the Crosslinked Am-6F-SPAEK/Am-SPAEK-H Blend Membranes

2.3.1. Epoxy-Crosslinked SPAEK Membranes

The epoxy-crosslinked SPAEK membranes using RDGE as crosslinker were prepared via a solution-casting method. The calculated weights of Am-6F-SPAEK, Am-SPAEK-H and RDGE were dissolved in DMSO at room temperature to prepare a 10 wt% solution. The molar ratio of epoxy groups on RDGE and amino groups on polymers was 1:1. The homogeneous solution was then filtered through 400-mesh cloth filter and cast onto clean leveled glass substrates. The membranes were dried at 80 °C for 12 h, 100 °C for 12 h and then in a vacuum oven at 120 °C for another 12 h. This series of membranes was then heated at 200 °C under vacuum conditions for 1 h for thermal activation of the crosslinking reaction between RDGE and aminated polymers.

The membranes were converted from salt form to acid form by immersing them in a 1 M sulfuric acid solution for 24 h, followed by washing membranes by immersing them in deionized water to wash the adsorbed acid for 24 h. After that, the membranes were stored in deionized water for further characterizations.

The epoxy-crosslinked Am-6F-SPAEK/Am-SPAEK-H blend membranes were referred to as EP-SPAEK−x, where x (x = 5, 10 and 15) represents the mass percentage of Am-SPAEK-H.

2.3.2. Silane-Crosslinked SPAEK Membranes

The silane-crosslinked SPAEK membranes were also prepared using a solution-casting method, and a simple treatment before casting was needed. The calculated weights of Am-6F-SPAEK and Am-SPAEK-H were firstly dissolved in DMSO to prepare a 5 wt% solution. A precalculated weight of GOPTS was added into the solution, and the solution was stirred at 80 °C under nitrogen protection for 12 h. Before casting, a few drops of concentrated hydrochloric acid were added into the solution. After stirring for 2 h, the mixtures were poured onto a clean glass through a 400-mesh cloth filter. The heating procedure was consistent with that of EP-SPAEK-x. This series of blend membranes was then immersed in 0.5 M sulfuric acid solution at 80 °C for 24 h to complete the hydrolysis of $–OCH_3$.

The silane-crosslinked Am-6F-SPAEK/Am-SPAEK-H blend membranes were referred to as SC-SPAEK−x, where x (x = 5, 10 and 15) represents the mass percentage of Am-SPAEK-H.

2.4. Characterization

The inherent viscosity was measured using an Ubbelohde viscometer in a water bath with a polymer concentration of 5 g/L in DMSO at 25 ± 0.1 °C. Fourier-transform infrared spectroscopy (FTIR) was conducted on a Nicolet Impact 410 Fourier-transform infrared spectrometer. ^{1}H NMR spectra were recorded on a Bruker Avance III 400 MHz spectrometer using DMSO-d6 as solvent.

The thermogravimetric analysis (TGA) was analyzed on a Perkin Elmer Pyris 1 TGA analyzer (PerkinElmer U.S. LLC., Shelton, CT, USA). The dry membranes were obtained by drying the as-prepared crosslinked membranes in a vacuum oven at 60 °C for 24 h to remove residual solvent and moisture. Before analysis, the dry samples were kept in the TGA furnace at 120 °C under a nitrogen atmosphere for at least 20 min to remove absorbed moisture. The samples were cooled to 80 °C and then reheated to 800 °C at 10 °C/min under a stream of nitrogen, and the temperatures at 5% weight loss were recorded for each sample.

The mechanical properties of the wet membranes were investigated using the Shimadzu AG-I 1KN instrument (Shimadzu Asia Pacific, Singapore) at a constant crosshead

speed of 2 mm/min. The size of samples was 15 mm × 5 mm. Before testing, the wet samples were obtained by immersing them in water for at least 48 h.

The atomic force microscope (AFM) analysis was done using the Dimension Icon AFM from Bruker in peak-force tapping mode.

2.5. Water Uptake (WU) and Swelling Ratio Measurements of the Membranes

The dry membranes were cut into a specific size (10 mm × 30 mm), and the weights and lengths of the candidate samples were accurately measured. Samples were immersed in deionized water at every desired temperature for 2 h. The weights and lengths of the films were quickly measured after wiping the water of the surface.

The water uptake (%) of a membrane was calculated from the following equation:

$$\text{Water uptake} = (m_1 - m_0)/m_0 \times 100\% \quad (1)$$

where m_1 (g) and m_0 (g) were the mass of wet and dry membrane samples, respectively.

The swelling ratio (%) was calculated by using the following relations:

$$\text{Swelling ratio} = (l_1 - l_0)/l_0 \times 100 \quad (2)$$

where l_1 (mm) and l_0 (mm) represent the lengths of wet and dry membrane samples, respectively.

2.6. Oxidative Stability

The oxidative stability of the membranes was assessed using the Fenton test, in which the samples were immersed in Fenton's reagent (3% H_2O_2 aqueous solution containing 2 ppm $FeSO_4$) at 80 °C. The stability was quantified based on two metrics: (1) the residual weight of the membrane after 12 h of exposure, and (2) the time elapsed until the sample began to disintegrate in the reagent. Each measurement was performed in duplicate, and the reported values represent the average of the two independent tests.

2.7. Gel Fraction

The gel fraction of the crosslinked membranes was calculated from the residue after repeatedly reflux-extracted with DMF by the Soxhlet extractor for 24 h. The insoluble part was dried at 120 °C under vacuum for 24 h and weighted. The gel fraction of the crosslinked membranes was calculated according to the following equation:

$$\text{Gel fraction} = m_3/m_2 \times 100\% \quad (3)$$

where m_2 (g) is the weight of the initial sample and m_3 (g) is the weight of the insoluble part after extraction from DMF.

2.8. Ion Exchange Capacity (IEC) of Membranes

The theoretical IEC of the crosslinked membranes was calculated based on the definition of IEC, which is the number of millimoles of sulfonic acid groups per gram of dry membrane. For each blend composition, the total amount of sulfonic acid groups was determined from the IEC and mass fraction of the sulfonated polymer components (Am-SPAEK-H and Am-6F-SPAEK). The theoretical IEC was then obtained by dividing the total millimoles of sulfonic acid groups by the total mass of the membrane, including the crosslinking agent. The calculation follows the equation

$$\text{Theoretical IEC} = (w_a \times IEC_a + w_b \times IEC_b)/(w_a + w_b + w_c)$$

where w is the mass fraction of each component in the membrane formulation, and the subscripts a, b, and c correspond to Am-SPAEK-H, Am-6F-SPAEK, and the crosslinking agent, respectively. This approach accounts for the fact that the crosslinking agent contributes to the total mass of the membrane but does not contain ion exchange groups, thereby reducing the overall IEC per gram of the final crosslinked membrane.

The experimental IEC values of pure and crosslinked membranes were determined using the classical titration method. The dry membranes were immersed in 2 mol/L NaCl solution for at least 24 h to exchange the H^+ ions in the membranes with Na^+ ions. The replaced protons within the solutions were titrated with 4 mmol/L NaOH aqueous solution using phenolphthalein as an indicator.

2.9. Proton Conductivity

The proton conductivity measurements were conducted through four-point alternating current impedance spectroscopy from 0.1 Hz to 100 kHz at 10 mV ac perturbation and 0 V dc rest voltage using a Princeton Applied Research Model 273A Potentiostat (Model 5210 frequency response detector, EG&G PARC, Princeton, NJ, USA).The membrane samples of 1 cm width and 6 cm length were fixed in a measuring cell with two outer gold wires to feed current to the sample and two inner gold wires to measure the voltage drops. All the samples were mounted between two Teflon plates. The cell was placed in deionized water for measurement. Prior to the measurements, the membranes were fully hydrated in water for 24 h. The proton conductivity (σ, S cm^{-1}) was calculated from the impedance data according to the following equation:

$$\sigma = l/(R \times A) \quad (4)$$

where l is the distance between the two electrodes (l = 1 cm), R (Ω) is the resistance of the membrane and A (cm^2) is the cross-sectional area of membrane.

2.10. DMFC Performance

The membrane electrode assembly (MEA) for fuel cell testing was manufactured with reference to the previously reported method [36]. Before testing, the SPAEK resin was dissolved in DMF to prepare a polymer solution with a mass concentration of 0.5% as the catalyst ink. The catalyst platinum powder was ultrasonically mixed with the prepared catalyst ink. After complete dispersion, the catalyst ink was sprayed evenly onto the carbon paper with a spray gun to form a gas diffusion electrode. The SPAEK film was hot-pressed between two electrodes, and then assembled into a single cell for testing. The loading amount of platinum in the catalyst layer was about 0.6 mg/cm^2, the test effective area was 9 cm^2, the test temperature was set at 40 °C, 60 °C and 80 °C, and the test fuel was methanol of different concentrations.

3. Results and Discussion

3.1. Syntheses of Am-6F-SPAEK and Am-SPAEK-H with Amino and Sulfonic Acid Groups

In this study, the structure features of the PAEKs are the simultaneous existence of basic amino groups and acidic sulfonic acid groups on one polymer. So far, only several such PAEKs with a high molecular weight have been synthesized by us and other research groups because complicated reactions from active amino groups may occur during the polymerizations or chemical modifications of polymers [34,36]. The multiple post-reactions of the existing polymers, such as sulfonation reactions [16,18], lithiation reactions [37,38], and bromination reactions [39], are applied to synthesize functionalized polymers with active groups. However, post-reactions sometimes lead to the decompositions of polymer backbones or some side effects. Another approach is to synthesize functionalized

polymers based on the polymerization of monomers with functional groups. Given the negative effects of the post-reactions, we adopted the second method to obtain two kinds of PAEKs with both amino groups and sulfonic acid groups through an aromatic nucleophilic substitution polycondensation (Scheme 1). The contents of functional -NH_2 groups and -SO_3H groups could be adjusted according to the feed ratios of bisphenols and difluoro-monomers. To weaken the strong "base–acid" interactions between -NH_2 groups and -SO_3H groups, the sulfonated difluoro-monomer in -SO_3Na form was used. Finally, the moderate-IEC SPAEK containing -CF_3 and -NH_2 groups (Am-6F-SPAEK) was obtained as a matrix, and the high-IEC SPAEK containing -NH_2 groups (Am-SPAEK-H) was achieved as a "performance-enhancing" component. It was noticed that Am-SPAEK-H was even dissolved in water due to its extremely high content of sulfonic acids (IEC~3.47 meq/g). The hydrophobic fluorine-containing moieties of Am-6F-SPAEK were expected to improve the membrane's stability under humidity circumstances, and the amino groups of the two polymers would serve as the reactive groups with the crosslinkers.

The chemical structures of the resulting Am-6F-SPAEK and Am-SPAEK-H were confirmed via ^{1}H NMR and FTIR spectroscopies. As shown in Figure 1, the ^{1}H NMR spectra of the two polymers exhibited signals of aromatic protons at 5.0–8.5 ppm, and all of the signals were properly assigned to the supposed chemical structure. The typical signals at about 5.33 ppm of the two polymers were caused by amine protons. The peaks at about 8.27 ppm were attributed to the hydrogen atoms (H3 and H3′) in the ortho position to the sulfonic acid groups of the two polymers.

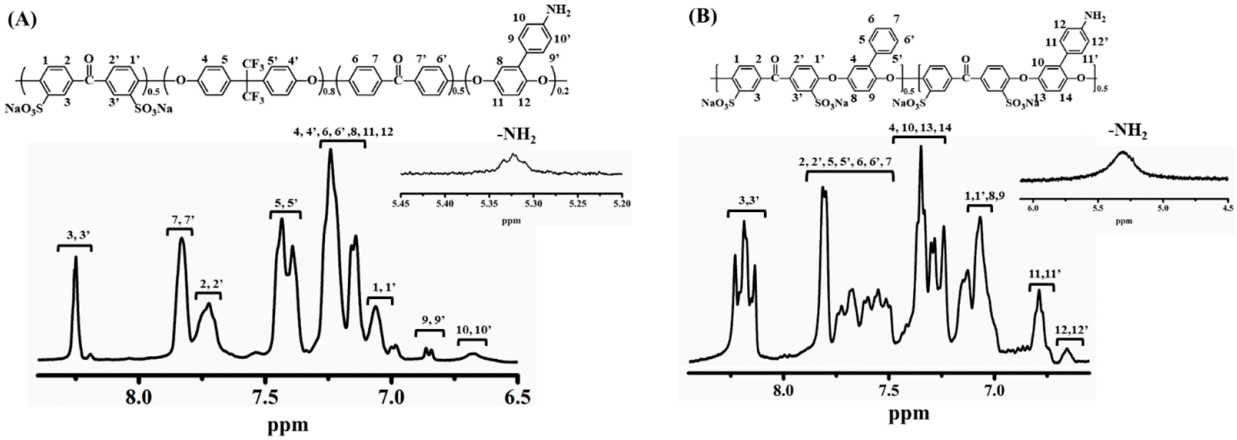

Figure 1. ^{1}H NMR spectra of Am-6F-SPAEK (**A**) and Am-SPAEK-H (**B**).

The FTIR spectra in Figure 2 clearly exhibit all characteristic absorptions corresponding to the designed functional groups, confirming the successful synthesis of the sulfonated and aminated PAEKs. The broad band at approximately 3380 cm^{-1} is attributed to N–H stretching of the primary amine (–NH_2) groups, while the strong peak at 1169 cm^{-1} corresponds to the Ar–O–Ar ether linkage of the PAEK backbone. The carbonyl (C=O) stretching vibration of the ketone group appears at 1655 cm^{-1}. Importantly, the presence of sulfonic acid (–SO_3H) groups is evidenced by the asymmetric S=O stretching at 1240 cm^{-1} and symmetric S=O stretching vibrations at 1082 and 1025 cm^{-1}. The coexistence of these distinct absorptions confirms the structural integrity of the dual-functionalized polymers, providing a firm basis for subsequent membrane fabrication and performance evaluation.

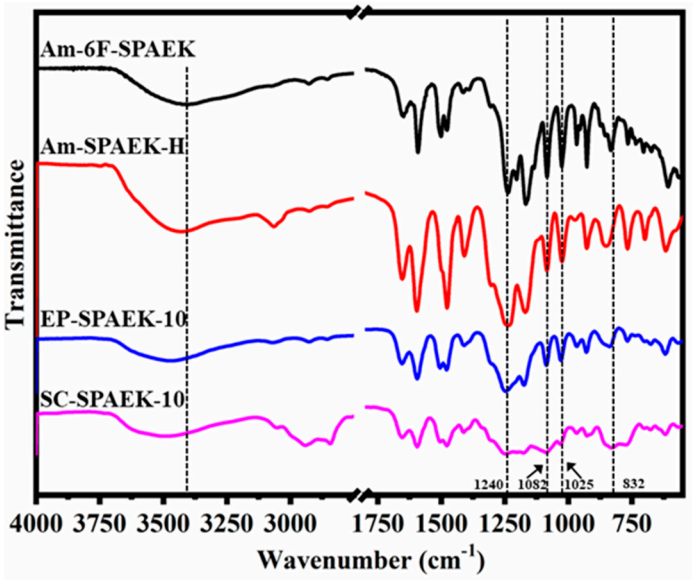

Figure 2. FTIR spectra of Am-6F-SPAEK, Am-SPAEK-H, EP-SPAEK−10 and SC-SPAEK−10.

3.2. Construction of Epoxy-Crosslinked and Silane-Crosslinked SPAEK Networks

An ideal PEM model is composed of a stable framework to maintain good mechanical strength and a functional microphase for proton transport and water storage. In this study, two chemically crosslinked networks having abundant -SO_3H groups were constructed. By using the highly efficient reaction of amino and epoxy groups, two series of crosslinked SPAEK-based membranes were fabricated via a common solution-casting procedure, followed by simple post-treatment. Different from the epoxy-crosslinked SPAEK membranes, silane-crosslinked ones could introduce the polysilsesquioxane component into networks. The existence of hydrophilic crosslinking components may be helpful for improvements in water uptakes and proton conducting.

As shown in Figure 2, FTIR spectroscopy was applied to characterize the chemical structure of crosslinked blend membranes. Strong absorption bands around 1240, 1082 and 1025 cm^{-1} were assigned to the symmetric and asymmetric stretching vibrations of O=S=O groups. These observations confirmed that sulfonic acid groups existed in the crosslinked membranes. Compared with the FTIR spectrum of EP-SPAEK−10, a new band at 832 cm^{-1} corresponding to the Si-O stretching vibration of SC-SPAEK−10 appeared, indicating a successful introduction of organic polysiloxane.

3.3. Solubility Behaviors, Gel Fraction Test and Oxidative Stability

In all cases, the strong and flexible blend membranes could be obtained through solution-casting from the homogeneous mixture solution of SPAEK polymers and crosslinkers, as illustrated in Figure 3. It was believed that the high-molecular-weight Am-6F-SPAEK matrix could provide enough strength and flexibility to maintain their mechanical integrity. A comparative experiment about the dissolving states in DMSO was conducted to check the resistance to solvents of the crosslinked membranes. After treatment in DMSO for 12 h, the Am-6F-SPAEK pristine membrane was dissolved into DMSO to form a solution. On the contrary, EP-SPAEK−10 and SC-SPAEK−10 blend membranes effectively maintained their shapes because of the stable crosslinked structure.

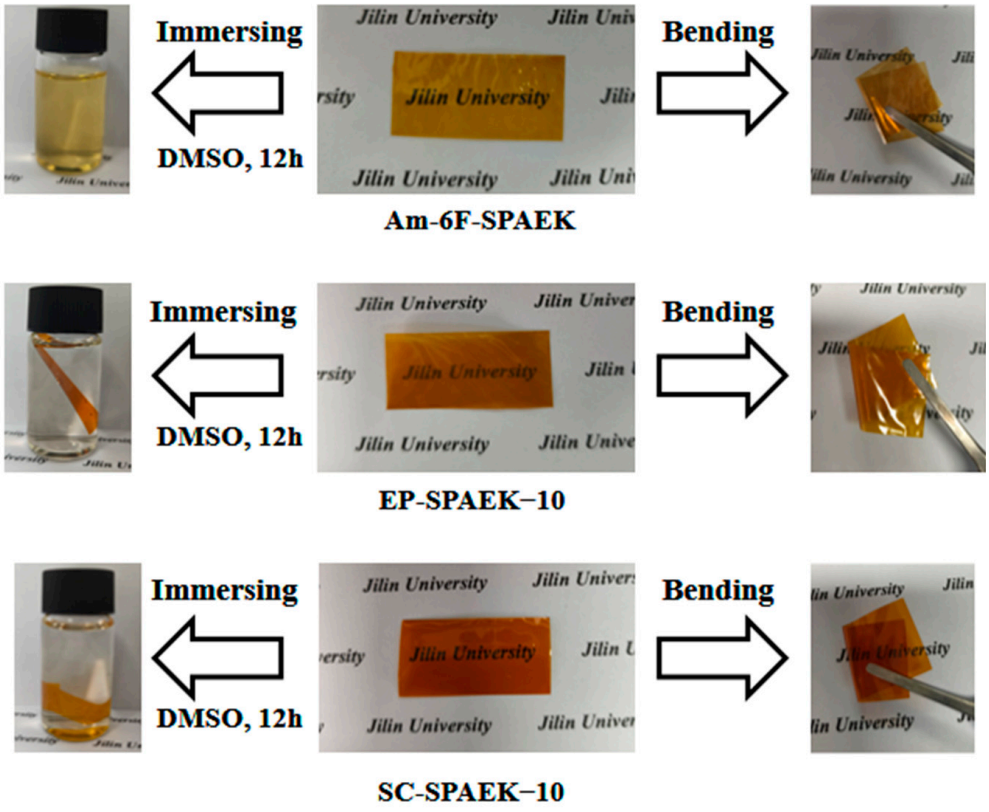

Figure 3. The photographs of membranes and their dissolving states in DMSO.

Measuring the solubility of membranes is a common method for evaluating the crosslinking effect. At room temperature, Am-6F-SPAEK and Am-SPAEK-H are soluble in some polar aprotic solvents, such as DMF, DMAc, NMP and DMSO. In comparison, all the obtained EP-SPAEK−5,10,15 and SC-SPAEK−5,10,15 membranes could not be dissolved in solvents even on heating, suggesting the formation of highly crosslinked networks. As given in Table 1, the gel contents of all the crosslinked blend membranes were higher than 84%. In particular, gel contents of the EP-SPAEK-x series were in the range of 95–96%, which were much higher than the 84–89% of the SC-SPAEK−x series. This indicated a stronger crosslinking capacity of the bis-epoxy crosslinker.

Table 1. Solubility and gel fraction of membranes.

Membrane	Oxidative Stability		IEC [c] (mmol/g)	IEC [d] (mmol/g)	Gel Fraction (%)
	RW (%) [a]	t (h) [b]			
Am-6F-SPAEK	88 ± 2	4.0 ± 0.3	1.71	1.69	-
EP-SPAEK−5	98 ± 1	6.0 ± 0.2	1.82	1.76	95 ± 0.5
EP-SPAEK−10	98 ± 1	6.0 ± 0.2	2.00	1.95	96 ± 1
EP-SPAEK−15	95 ± 0.5	6.0 ± 0.2	2.17	2.10	96 ± 0.5
SC-SPAEK−5	95 ± 0.5	4.5 ± 0.5	1.74	1.70	84 ± 2
SC-SPAEK−10	96 ± 2	4.0 ± 1.0	1.91	1.91	89 ± 2
SC-SPAEK−15	92 ± 2	4.0 ± 0.3	2.07	2.05	87 ± 1

[a] Retained weights of samples after immersing in Fenton's reagent for 1 h. [b] The dissolved time of samples. [c] Theoretical value. [d] Experimental value.

Oxidative stability is an important indicator to evaluate whether the materials can withstand the strong oxidizing environment during the fuel cell operation. In this study, the time that the samples start to break into pieces in Fenton's reagent at 80 °C and the retained weight after treatment in Fenton's reagent at 80 °C for 1 h were recorded to assess

the oxidative stability (Table 2). Obviously, the crosslinked EP-SPAEK-x (RW~96–98%) and SC-SPAEK-x (RW~92–96%) blend membranes had higher retained weights than the Am-6F-SPAEK pristine membrane, suggesting their good oxidative stability. It was noticed that at the same crosslinker doping level, the EP-SPAEK-x series even showed a longer broken time and a higher retained weight in comparison to SC-SPAEK-x ones. The improved oxidative stability of EP-SPAEK-x membranes may be related to their highly crosslinked networks and stable molecular structure. The oxidative stability of the samples prepared in this study is found to be comparable with the values reported in the literature for analogous base resin systems [40,41].

Table 2. Water uptake, swelling ratio, conductivity and mechanical property of membranes.

Membrane	Water Uptake (%)		Swelling Ratio (%)		Conductivity (mS/cm)		Tensile Strength (MPa)	Elongation at Break (%)
	80 °C	100 °C	80 °C	100 °C	80 °C	100 °C		
Am-6F-SPAEK	29.5	31.3	11.4	13.1	67.6	96.9	26.4	17.3
EP-SPAEK−5	30.2	32.5	12.4	14.0	74.4	120.0	33.6	22.3
EP-SPAEK−10−10	42.4	46.9	12.8	14.2	93.3	156.3	30.0	31.5
EP-SPAEK−15	42.9	47.2	12.8	14.3	106.5	184.5	28.8	20.1
SC-SPAEK−5	30.7	36.5	12.6	13.2	76.0	127.3	41.7	15.3
SC-SPAEK−10−10	42.1	47.2	13.7	14.7	116.6	179.5	37.4	9.8
SC-SPAEK−15	42.4	53.9	14.0	14.9	118.5	187.6	35.7	16.4
SPAESK-15 [42]	85.6	146.5	-	49.3	-	181.5	43.7	43.4
C-SPAEKS/ NGO-0.75 [40]	23.02	-	17.34	-	-	171.1 (90 °C)	21.4	12.7
S-Am-2.0/C [41]	14.6	-	4.87	-	135	-	36.1	7.6

3.4. Thermal and Mechanical Properties

The TGA results (Figure 4) confirm that both epoxy- and silane-crosslinked membranes retain the characteristic two-stage degradation profile of SPAEK-based materials. The initial weight loss (200–350 °C) corresponds to the desulfonation and decomposition of aliphatic crosslinker segments, while the major backbone degradation occurs above 450 °C. The silane-crosslinked membranes display a marginally earlier onset of the first degradation step, which can be attributed to the presence of the less thermally stable aliphatic chains derived from the GOPTS crosslinker. Nevertheless, all crosslinked membranes maintain a 5 wt% loss temperature above 300 °C and demonstrate negligible decomposition below 200 °C. This thermal behavior comfortably meets the operational requirements of PEMFCs and DMFCs (typically $\leq$ 100 °C), confirming the practical thermal stability of the designed crosslinked networks.

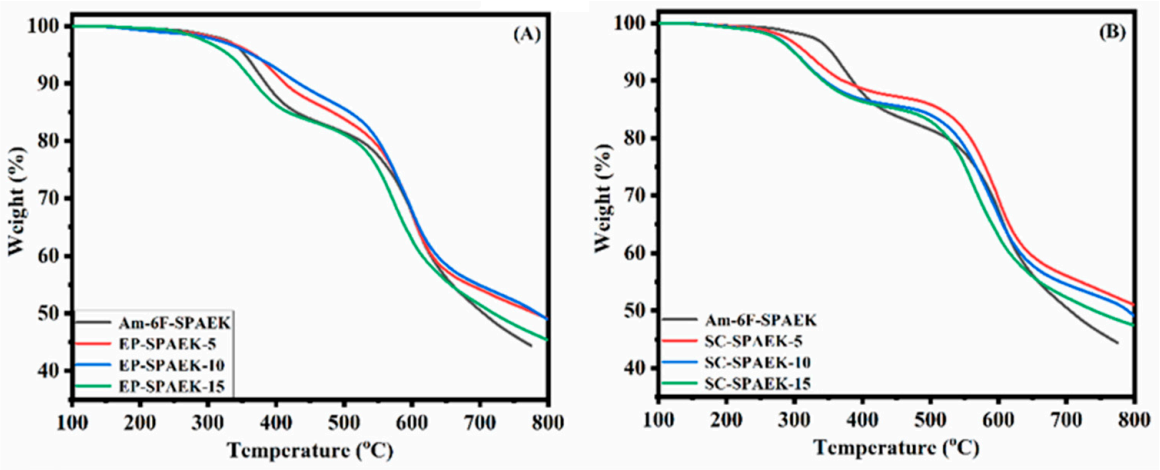

Figure 4. TGA curves of the two series of membranes under N_2. TGA curves measured under nitrogen atmosphere for two series of membranes. (**A**) EP-SPAEK−x series; (**B**) EP-SPAEK−x series.

An adequate mechanical strength is necessary for PEMs to withstand a fabrication process of membrane electrode assemblies (MEAs) and long-term service in fuel cells. Tensile strengths, along with elongations at break of the membranes, are summarized in Table 2. As expected, the crosslinked blend membranes exhibited a higher tensile strength of 28.81–41.66 MPa than the 26.43 MPa of the pristine membrane. The improvements in the strengths could be explained by the formation of stable crosslinked networks. Meanwhile, the elongations at break of the crosslinked blend membranes were 9.79–31.47%. For EP-SPAEK-x membranes, the values of both strengths and elongations at a break were superior to those of the pristine membrane, indicating their more reasonable structure.

3.5. Morphology Study

The hydrophilic–hydrophobic phase-separated structure is generally considered to be potentially linked to proton conduction performance. The microscopic morphology of the pristine Am-6F-SPAEK and SC-SPAEK−10 samples was characterized by the tapping mode AFM to get a good understanding of surface morphology after modification. As shown in Figure 5, compared with the pristine membrane, SC-SPAEK−10 exhibits more clearly defined bright regions in the AFM phase images. This indicates enhanced hydrophilic–hydrophobic phase separation, rather than simply an increase in the number of hydrophilic domains. The improved contrast and definition suggest the formation of more well-developed hydrophilic microdomains, which could provide continuous pathways favorable for proton transport.

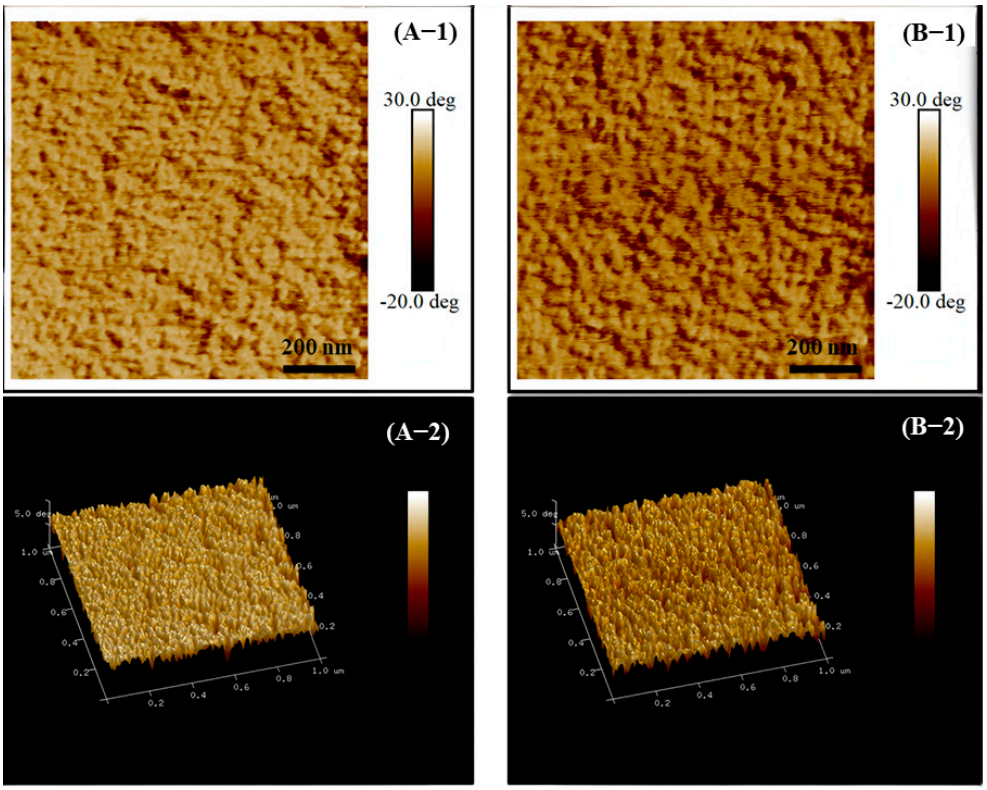

Figure 5. AFM phase images of membranes. (**A-1**,**A-2**) Am-6F-SPAEK membrane; (**B-1**,**B-2**) SC-SPAEK−10 membrane. (**A-1**,**B-1**) Two-dimensional phase images; (**A-2**,**B-2**) Three-dimensional topography phase images.

3.6. Water Uptake and Swelling Ratio

Water uptake (WU) and dimensional swelling ratio (SR) are two key parameters related to the proton conductivity and dimensional stability of the PEMs. Usually, a preferred membrane is required to have suitable WU and low swelling to maintain sufficient proton conductivity without over-swelling. In the current study, stable crosslinked SPAEK networks with a high-IEC component were expected to achieve a good balance between WU and SR. As illustrated in Figure 6A,B, it was obvious that the incorporation of a high-IEC SPAEK component played a positive role in the increase in water uptake, and all the blend membranes had higher WU values than the pristine membrane. Notably, at equivalent Am-SPAEK-H content, the SC-SPAEK-x series displayed higher WU than its EP-SPAEK-x counterpart, which can be attributed to the presence of additional hydrophilic Si–OH groups generated from hydrolysis of the silane crosslinker.

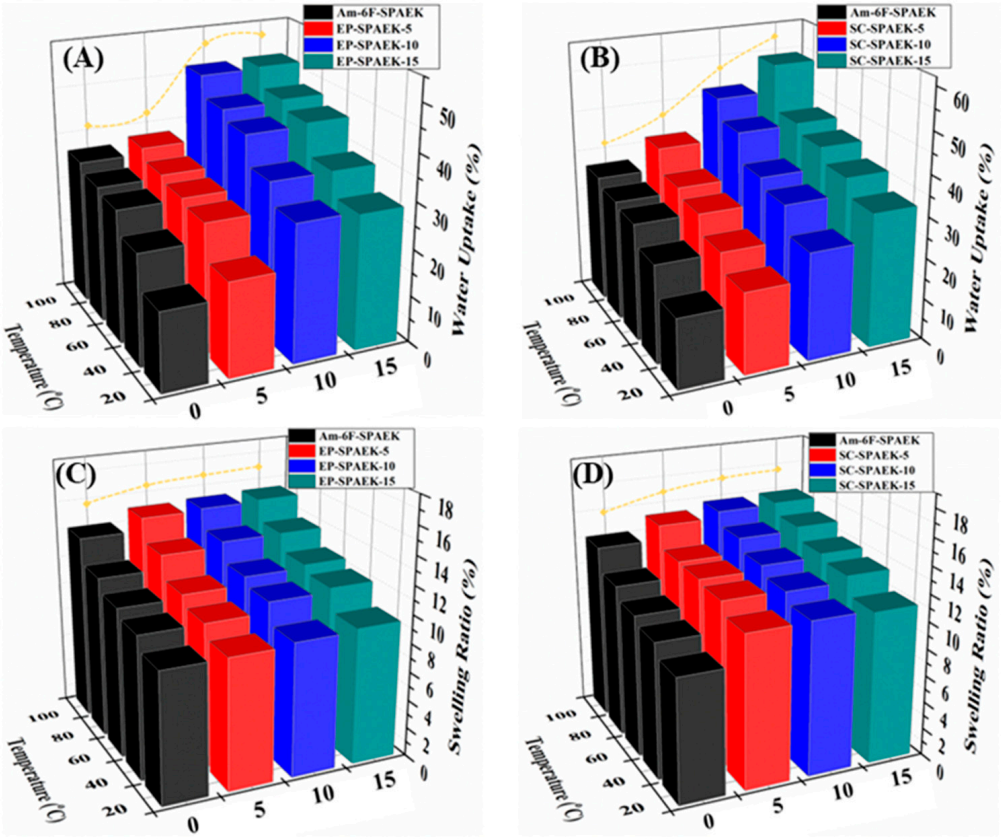

Figure 6. Water uptakes (**A**,**B**) and swelling ratios (**C**,**D**) of the prepared membranes tested at different temperatures. (**A**) Water uptake of EP-SPAEK−x series membranes; (**B**) Water uptake of SC-SPAEK−x series membranes; (**C**) Swelling ratio of EP-SPAEK−x series membranes; (**D**) Swelling ratio of SC-SPAEK−x series membranes.

Importantly, both crosslinked blend membrane systems exhibited markedly suppressed swelling behavior, as confirmed in Figure 6C,D. Even at 100 °C, all crosslinked membranes maintained SR values below 15%, substantially lower than those reported for many conventional SPAEK-based membranes. Despite the incorporation of the high-IEC component, the crosslinked blends showed only marginal increases in SR compared to the pristine membrane. This exceptional dimensional stability is ascribed to the robust crosslinked network structure, which effectively restrains polymer chain expansion upon hydration. Notably, the swelling behavior also shows a temperature-dependent trend with composition. At 80 °C, the swelling ratio exhibits a minimum at intermediate Am-SPAEK-H content. This behavior is attributed to the balance between crosslink density

and hydrophilic/hydrophobic interactions: the crosslinked network restricts macroscopic swelling, while the introduced hydrophilic groups promote water uptake, leading to the observed minimum. At 100 °C, however, the increased thermal energy weakens these interactions and accelerates water absorption, resulting in a monotonic increase in swelling with increasing hydrophilic content. This temperature-dependent behavior is consistent with typical trends reported in similar crosslinked polymer systems. In summary, the crosslinking strategy implemented in this study successfully decouples the typically competing properties of water uptake and dimensional swelling. The formed stable network enables enhanced proton conduction through controlled water retention while significantly mitigating excessive swelling, thereby demonstrating a promising approach to advancing PEM performance for fuel cell applications.

3.7. Proton Conductivity

The main goal of this study is to prepare high-conductivity membranes with essential dimensional and mechanical integrity. In most cases, high conductivity depends on a high concentration of -SO_3H groups, which also facilitates the formation of "proton conducting channels". The incorporation of high-IEC SPAEK effectively increased the IEC values from 1.69 mmol/g (Am-6F-SPAEK) to 2.10 mmol/g (EP-SPAEK-15) and 2.05 mmol/g (SC-SPAEK-15), respectively. Consequently, the performance-enhanced blend membranes exhibited a continuous increase in proton conductivity with increasing high-IEC SPAEK loading (Figure 7). At 100 °C, the maximum proton conductivities of EP-SPAEK-15 and SC-SPAEK-15 reached 0.1845 S/cm and 0.1876 S/cm, respectively. For comparison, the proton conductivity of the pristine Am-6F-SPAEK membrane was only 0.0969 S/cm under the same test conditions. It should be noted that the slight change in the slope of the proton conductivity–temperature profile is not ascribed to an intrinsic phase transition of the membrane material, but is likely an experimental artifact related to the heating rate during measurement. All samples were tested under identical heating conditions to ensure the reliability and comparability of the data. Notably, at similar IEC levels, the SC-SPAEK-x series exhibited relatively higher conductivity than the EP-SPAEK-x series. This phenomenon can be attributed to their higher water absorption, which is associated with the strong hydrophilicity of Si-O-Si-OH moieties.

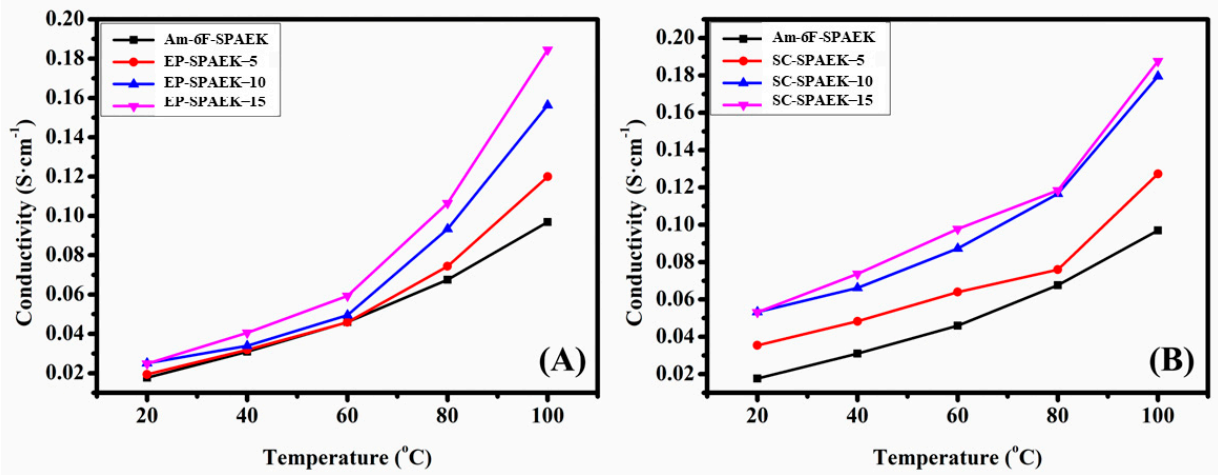

Figure 7. Proton conductivities of the prepared membranes measured at varying temperatures. (**A**) Am-6F-SPAEK, EP-SPAEK−5, EP-SPAEK−10 and EP-SPAEK−15 membranes; (**B**) Am-6F-SPAEK, SC-SPAEK−5, SC-SPAEK−10 and SC-SPAEK−15 membranes.

3.8. Single-Fuel-Cell Performance of the Membranes

Given their superior comprehensive properties, the membranes with x = 10 (including EP-SPAEK−10 and SC-SPAEK−10) were selected for single-fuel-cell testing. Compared with x = 5 and x = 15 samples, the x = 10 membranes achieved an optimal balance of properties that are critical for long-term fuel cell operation. While the mechanical strength differences between the x = 10 and x = 15 membranes are small, the x = 10 membranes exhibit significantly higher oxidative stability, as evidenced by their longer oxidation resistance time and lower residual weight loss in Fenton's test. This enhanced oxidative stability is a decisive advantage for mitigating radical-induced degradation, a major failure mechanism in DMFCs. In addition, the x = 10 membranes show a well-balanced combination of ion exchange capacity (IEC), dimensional stability, and mechanical robustness, making them the most practically relevant candidates for DMFC operation. Therefore, MEAs were fabricated using the EP-SPAEK−10 and SC-SPAEK−10 membranes, with the Am-6F-SPAEK membrane tested as a reference. DMFC polarization curves were successfully obtained at different temperatures, as shown in Figure 8. The anode was supplied with 1 M and 4 M methanol solutions, respectively. Under all test temperatures and methanol concentrations, both EP-SPAEK−10 and SC-SPAEK−10 exhibited improved electrochemical performance compared to the reference membrane. For all membranes, the power density increased sequentially with temperature: 40 °C < 60 °C < 80 °C. When the methanol concentration increased from 1 M to 4 M, the maximum power density of all three membranes showed a corresponding rise. At 80 °C with 1 M methanol, the maximum power densities of Am-6F-SPAEK, EP-SPAEK−10, and SC-SPAEK−10 were 8.48, 16.67, and 29.94 mW cm^{-2}, respectively (Table 3). At 80 °C with 4 M methanol, the highest power density of SC-SPAEK−10 reached 31.67 mW cm^{-2}, which was nearly three times higher than the 10.77 mW cm^{-2} of Am-6F-SPAEK. A key challenge in proton exchange membrane design is the trade-off between water uptake and swelling. In this work, our crosslinked network addresses this issue through a positive decoupling effect. The crosslinking structure effectively restricts the macroscopic swelling of the membrane, while the introduced high-IEC SPAEK domains provide abundant water retention sites. As a result, the membrane maintains high water uptake for proton conduction while exhibiting low swelling for dimensional stability. This unique combination is critical to the enhanced performance observed in DMFC tests. This significant improvement in cell performance is closely attributed to the excellent overall properties of the silane-crosslinked SPAEK membrane, including high proton conductivity, good mechanical strength, and low swelling ratio.

Table 3. DMFC performance of Am-6F-SPAEK, EP-SPAEK−10 and SC-SPAEK−10.

Membrane	OCV (V)			PD_{Max} (mW/cm^2)		
	40 °C	60 °C	80 °C	40 °C	60 °C	80 °C
Am-6F-SPAEK (1 M)	0.91	0.62	0.68	4.48	6.36	8.48
Am-6F-SPAEK (4 M)	0.59	0.61	0.61	4.34	10.93	10.77
EP-SPAEK−10 (1 M)	0.70	0.59	0.63	7.48	10.43	16.67
EP-SPAEK−10 (4 M)	0.66	0.65	0.63	15.24	17.44	16.67
SC-SPAEK−10 (1 M)	0.62	0.77	0.65	14.08	21.61	29.94
SC-SPAEK−10 (4 M)	0.66	0.58	0.59	15.83	31.44	31.67

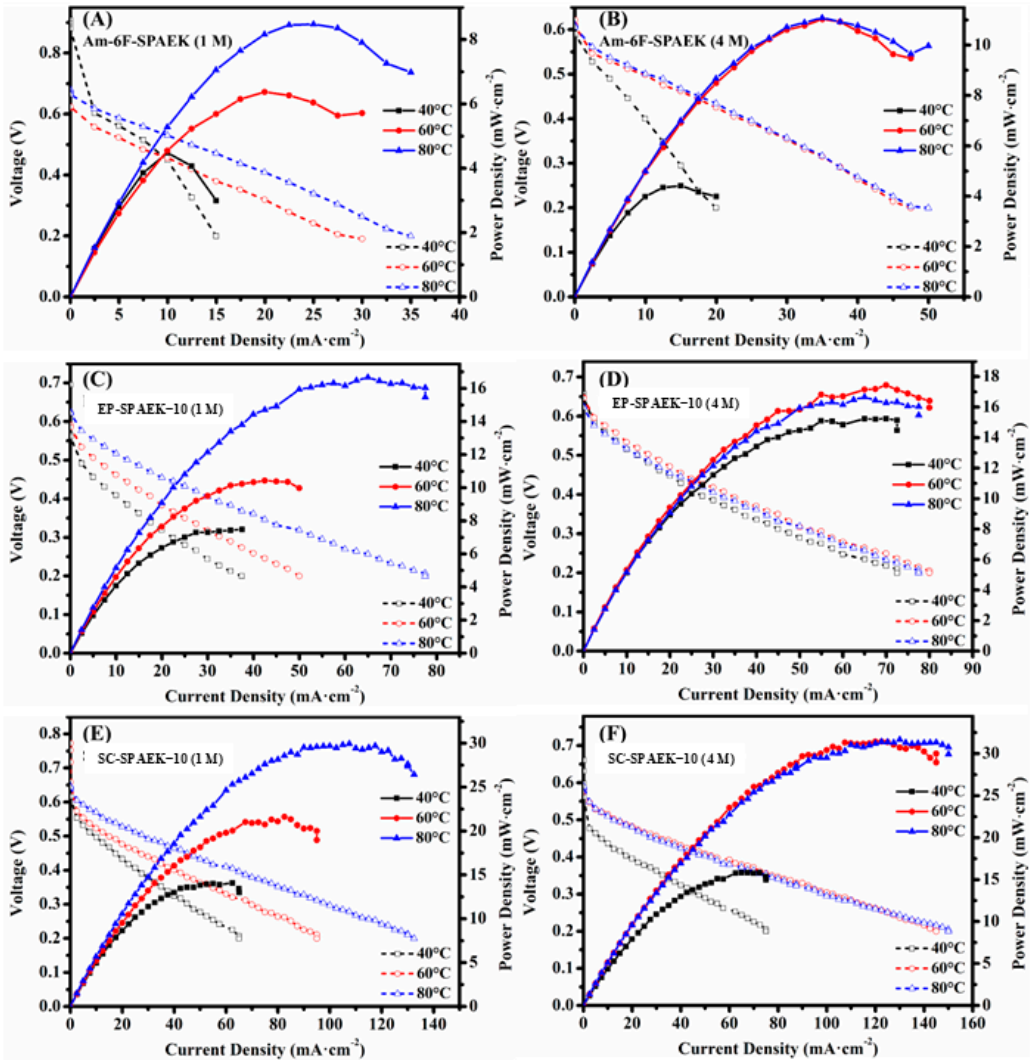

Figure 8. DMFC performance of Am-6F-SPAEK, EP-SPAEK−10 and SC-SPAEK−10 membranes measured at different temperatures; open symbols represent polarization curves, and filled symbols represent power density curves. (**A**) Am-6F-SPAEK (1 M); (**B**) Am-6F-SPAEK (4 M); (**C**) EP-SPAEK−10 (1 M); (**D**) EP-SPAEK−10 (4 M); (**E**) SC-SPAEK−10 (1 M); (**F**) SC-SPAEK−10 (4 M).

4. Conclusions

Based on the successful synthesis of amine- and sulfonate-functionalized poly(aryl ether ketone)s, two chemically crosslinked blend networks were systematically constructed in this study by combining a moderate-IEC fluorine-containing SPAEK with a high-IEC SPAEK through a solution-casting process. This work establishes a platform for investigating structure–property relationships in crosslinked polyelectrolyte membranes. The high-IEC SPAEK was demonstrated to serve as a "performance-enhancing component," playing a crucial role in improving proton conductivity and water management. Both epoxy- and organosilicon-crosslinked SPAEK membranes exhibited exceptionally high proton conductivities exceeding 0.18 S cm^{-1} at 100 °C, along with favorable mechanical strength and low swelling. Notably, the two crosslinking strategies show distinct advantages: epoxy-based crosslinking provides excellent long-term stability, making it preferable for applications requiring high durability, while silane-based crosslinking achieves higher proton conductivity, which is more suitable for high-performance scenarios prioritizing power output. When fabricated into MEAs, EP-SPAEK−10 and SC-SPAEK−10 showed enhanced DMFC performance compared to the reference membrane. Specifically, the

SC-SPAEK−10 membrane achieved a maximum power density of 31.67 mW cm^{-2}, which represents a several-fold increase over that of Am-6F-SPAEK. Overall, this work establishes a clear connection between crosslinking structure and performance, thereby providing a guiding principle for the rational design of high-performance membranes for next-generation fuel cells. Future work will focus on developing hybrid crosslinked networks that combine the benefits of both strategies to further balance stability and conductivity.

Author Contributions: Conceptualization, B.L. (Baijun Liu); Methodology, Z.L. and B.L. (Bing Liang); Formal analysis, Z.L. and B.L. (Bing Liang); Investigation, Z.L.; Data curation, Z.X.; Writing—original draft, Z.L.; Writing—review and editing, B.L. (Baijun Liu); Visualization, Z.X.; Supervision, W.H. and B.L. (Baijun Liu); Project administration, B.L. (Baijun Liu); Funding acquisition, B.L. (Baijun Liu). All authors have read and agreed to the published version of the manuscript.

Funding: This research was funded by the National Natural Science Foundation of China, grant numbers 52573009 and 52073118.

Data Availability Statement: The original contributions presented in this study are included in the article. Further inquiries can be directed to the corresponding author.

Acknowledgments: The authors are grateful for the financial support provided by the National Natural Science Foundation of China.

Conflicts of Interest: The authors declare no conflict of interest.

References

1. Zong, X.; Wang, L.; Mi, H.; Liu, Y.; Li, J.; Liu, B.; Hu, W.; Cai, W.; Jiang, C. Porous aromatic framework with imidazole group reinforced high-temperature proton exchange membrane with promoted proton transport efficiency and power density. *ACS Sustain. Chem. Eng.* **2024**, *12*, 13326–13335.
2. Yang, J.; Shi, C.; Li, J.; Li, T.; Zhang, H.; Chen, Q.; Wang, P.; Hu, W.; Liu, B. Arylether-type polybenzimidazole-based composites containing imidazole-substituted heteropolyacid salts for high-temperature proton exchange membrane fuel cells. *Electrochim. Acta* **2025**, *511*, 145368. [CrossRef]
3. Peng, J.; Liang, M.; Liu, Z.; Wang, P.; Shi, C.; Hu, W.; Liu, B. Poly(arylene ether sulfone) crosslinked networks with pillar [5]arene units grafted by multiple long-chain quaternary ammonium salts for anion exchange membranes. *Chem. Commun.* **2020**, *56*, 928–931.
4. Paulus, N. Decarbonization potential of fuel cell technologies in micro-cogeneration applications: Spotlight on SOFCs in a belgian case study. *Prog. Energy* **2025**, *7*, 022005. [CrossRef]
5. Soo, L.K.; Sandip, M.; Seung, K.Y.; Kreller, C.R.; Wilson, M.S.; Larsen, D.; Elangovan, S.E.; Mukundan, R. Intermediate temperature fuel cells via an ion-pair coordinated polymer electrolyte. *Energy Environ. Sci.* **2018**, *11*, 979–987. [CrossRef]
6. Li, T.; Yang, J.; Chen, Q.; Zhang, H.; Wang, P.; Hu, W.; Liu, B. Construction of highly conductive cross-linked polybenzimidazole-based networks for high-temperature proton exchange membrane fuel cells. *Materials* **2023**, *16*, 1932. [CrossRef]
7. Won, S.D.; Guiver, M.D.; Moo, L.Y. Hydrocarbon-based polymer electrolyte membranes: Importance of morphology on ion transport and membrane stability. *Chem. Rev.* **2017**, *117*, 4759–4805. [CrossRef]
8. Wang, Y.; Shi, J.; Gu, X.; Deutschmann, O.; Shi, Y.; Cai, N. Toward mobility of solid oxide fuel cells. *Prog. Energy Combust. Sci.* **2024**, *102*, 101141. [CrossRef]
9. Wang, F.; Lv, J.; Liu, S.; Zhao, C.; Li, N.; Hu, Z.; Chen, S. Sulfonated polyhedral oligomeric sesquioxane-modified eptfe/sulfonated poly(ether ether ketone) pore-filling proton exchange membranes for fuel cells. *J. Membr. Sci.* **2026**, *740*, 124958. [CrossRef]
10. Zhang, D.; Xin, L.; Xia, Y.; Dai, L.; Qu, K.; Huang, K.; Fan, Y.; Xu, Z. Advanced nafion hybrid membranes with fast proton transport channels toward high-performance vanadium redox flow battery. *J. Membr. Sci.* **2021**, *624*, 119047. [CrossRef]
11. Ru, C.; Gu, Y.; Duan, Y.; Zhao, C.; Na, H. Enhancement in proton conductivity and methanol resistance of nafion membrane induced by blending sulfonated poly(arylene ether ketones) for direct methanol fuel cells. *J. Membr. Sci.* **2019**, *573*, 439–447. [CrossRef]
12. Li, N.; Cui, Z.; Zhang, S.; Li, S.; Zhang, F. Preparation and evaluation of a proton exchange membrane based on oxidation and water stable sulfonated polyimides. *J. Power Sources* **2007**, *172*, 511–519. [CrossRef]
13. Zhang, G.; Qu, Z.; Tao, W.-Q.; Mu, Y.; Jiao, K.; Xu, H.; Wang, Y. Advancing next-generation proton-exchange membrane fuel cell in multi transfer. *Joule* **2024**, *8*, 45–63.

14. Tang, H.; Geng, K.; Hao, J.; Zhang, X.; Shao, Z.; Li, N. Properties and stability of quaternary ammonium-biphosphate ion-pair poly(sulfone)s high temperature proton exchange membranes for H2 /O2 fuel cells. *J. Power Sources* **2020**, *475*, 228521. [CrossRef]
15. Song, Y.; Jin, Y.; Liang, Q.; Li, K.; Zhang, Y.; Hu, W.; Jiang, Z.; Liu, B. Novel sulfonated polyimides containing multiple cyano groups for polymer electrolyte membranes. *J. Power Sources* **2013**, *238*, 236–244. [CrossRef]
16. Liu, B.; Gilles, R.; Dae-Sik, K.; Michael, G.; Hu, W.; Jiang, Z. Aromatic poly(ether ketone)s with pendant sulfonic acid phenyl groups prepared by a mild sulfonation method for proton exchange membranes. *Macromolecules* **2007**, *40*, 1934–1944. [CrossRef]
17. Zeng, W.; Guan, B.; Zhuang, Z.; Chen, J.; Zhu, L.; Ma, Z.; Hu, X.; Zhu, C.; Zhao, S.; Shu, K.; et al. Comprehensive review on the advances and comparisons of proton exchange membrane fuel cells (PEMFCs) and anion exchange membrane fuel cells (AFCS): From fundamental principles to key component technologies. *Int. J. Hydrogen Energy* **2025**, *102*, 222–246. [CrossRef]
18. Bae, B.; Miyatake, K.; Uchida, M.; Uchida, H.; Sakiyama, Y.; Okanishi, T.; Watanabe, M. Sulfonated poly(arylene ether sulfone ketone) multiblock copolymers with highly sulfonated blocks. Long-term fuel cell operation and post-test analyses. *ACS Appl. Mater. Interfaces* **2011**, *3*, 2786–2793. [CrossRef]
19. Gong, C.; Zheng, X.; Liu, H.; Wang, G.; Cheng, F.; Zheng, G.; Wen, S.; Law, W.-C.; Tsui, C.-P.; Tang, C.-Y. A new strategy for designing high-performance sulfonated poly(ether ether ketone) polymer electrolyte membranes using inorganic proton conductor-functionalized carbon nanotubes. *J. Power Sources* **2016**, *325*, 453–464. [CrossRef]
20. Cui, L.; Geng, Q.; Gong, C.; Liu, H.; Zheng, G.; Wang, G.; Liu, Q.; Wen, S. Novel sulfonated poly (ether ether ketone)/silica coated carbon nanotubes high-performance composite membranes for direct methanol fuel cell. *Polym. Adv. Technol.* **2015**, *26*, 457–464. [CrossRef]
21. Wang, C.; Lee, S.Y.; Shin, D.W.; Kang, N.R.; Lee, Y.M.; Guiver, M.D. Proton-conducting membranes from poly(ether sulfone)s grafted with sulfoalkylamine. *J. Membr. Sci.* **2013**, *427*, 443–450.
22. Xie, H.; Tao, D.; Xiang, X.; Ou, Y.; Bai, X.; Wang, L. Synthesis and properties of highly branched star-shaped sulfonated block poly(arylene ether)s as proton exchange membranes. *J. Membr. Sci.* **2015**, *473*, 226–236. [CrossRef]
23. Li, X.; Song, Y.; Liu, Z.; Feng, P.; Liu, S.; Yu, Y.; Jiang, Z.; Liu, B. Triple-layer sulfonated poly(ether ether ketone)/sulfonated polyimide membranes for fuel cell applications. *High Perform. Polym.* **2014**, *26*, 106–113. [CrossRef]
24. Feng, S.; Shen, K.; Wang, Y.; Pang, J.; Jiang, Z. Concentrated sulfonated poly (ether sulfone)s as proton exchange membranes. *J. Power Sources* **2013**, *224*, 42–49. [CrossRef]
25. Guo, M.; Li, X.; Li, L.; Yu, Y.; Song, Y.; Liu, B.; Jiang, Z. Novel postsulfonated poly(ether ether ketone)-block-poly(ether sulfone)s as proton exchange membranes for fuel cells: Design, preparation and properties. *J. Membr. Sci.* **2011**, *380*, 171–180. [CrossRef]
26. Liu, D.; Dong, B.; Zhang, H.; Xie, Y.; Pang, J.; Jiang, Z. High methanol resistant polyelectrolyte membrane based on semi-crystalline poly(ether ketone) with densely sulfonated side chain for direct methanol fuel cell. *J. Power Sources* **2021**, *482*, 228982. [CrossRef]
27. Zhu, M.; Song, Y.; Hu, W.; Li, X.; Jiang, Z.; Guiver, M.D.; Liu, B. Spaek-based binary blends and ternary composites as proton exchange membranes for dmfcs. *J. Membr. Sci.* **2012**, *415-416*, 520–526. [CrossRef]
28. Barjola, A.; Escorihuela, J.; Andrio, A.; Giménez, E.; Compañ, V. Enhanced conductivity of composite membranes based on sulfonated poly(ether ether ketone) (speek) with zeolitic imidazolate frameworks (zifs). *Nanomaterials* **2018**, *8*, 1042. [CrossRef]
29. Yavuz, Y.; Alpay, S.; Irfan, A. Effect of thermal crosslinking process on membrane structure and pem fuel cell applications performed with speek-pva blend membranes. *Int. J. Hydrogen Energy* **2022**, *47*, 40445–40461. [CrossRef]
30. Ramly, N.N.; Aini, N.A.; Sahli, N.; Aminuddin, S.; Yahya, M.; Ali, A. Dielectric behaviour of uv-crosslinked sulfonated poly (ether ether ketone) with methyl cellulose (speek-mc) as proton exchange membrane. *Int. J. Hydrogen Energy* **2016**, *42*, 9284–9292. [CrossRef]
31. Li, P.; Dang, J.; Wu, W.; Lin, J.; Zhou, Z.; Zhang, J.; Wang, J. Nanofiber composite membrane using quantum dot hybridized speek nanofiber for efficient through-plane proton conduction. *J. Membr. Sci.* **2020**, *609*, 118198. [CrossRef]
32. Liu, B.; Hu, W.; Robertson, P. Poly(aryl ether ketone)s with carboxylic acid groups: Synthesis, sulfonation and crosslinking. *J. Mater. Chem.* **2008**, *18*, 4675–4682. [CrossRef]
33. Aashika, R.C.; Sumi, K.; Prasath, J.; Arivanandhan, M. Bifunctional characteristics of vetiveria zizanioides incorporated pvdf polymer nanocomposite membrane for wastewater treatment and energy storage applications. *Chem. Eng. J.* **2025**, *516*, 163883. [CrossRef]
34. Guo, M.; Liu, B.; Li, L.; Liu, C.; Wang, L.; Jiang, Z. Preparation of sulfonated poly(ether ether ketone)s containing amino groups/epoxy resin composite membranes and their in situ crosslinking for application in fuel cells. *J. Power Sources* **2010**, *195*, 11–20. [CrossRef]
35. Wang, F.; Chen, T.; Xu, J. Sodium sulfonate-functionalized poly(ether ether ketone)s. *Macromol. Chem. Phys.* **1998**, *199*, 1421–1426. [CrossRef]
36. Guo, M.; Liu, B.; Liu, Z.; Wang, L.; Jiang, Z. Novel acid–base molecule-enhanced blends/copolymers for fuel cell applications. *J. Power Sources* **2009**, *189*, 894–901. [CrossRef]

37. Dai, Y.; Guiver, M.D.; Robertson, G.P.; Kang, Y.S.; Lee, K.; Jho, J.Y. Preparation and characterization of polysulfones containing both hexafluoroisopropylidene and trimethylsilyl groups as gas separation membrane materials. *Macromolecules* **2004**, *37*, 1403–1410. [CrossRef]
38. Lafitte, B.; Karlsson, L.E.; Jannasch, P. Sulfophenylation of polysulfones for proton-conducting fuel cell membranes. *Macromol. Rapid Commun.* **2002**, *23*, 896–900. [CrossRef]
39. Liu, Z.; Wang, P.; Hu, W.; Liu, B. Preparation and properties of hybrid silane-crosslinked sulfonated poly(aryl ether ketone)s as proton exchange membranes. *Chem. Res. Chin. Univ.* **2019**, *35*, 937–944. [CrossRef]
40. Feng, K.; Zhao, P.; Meng, L.; Xu, J.; Lei, J.; Li, N.; Chen, F.; Wang, J.; Shi, Q. Poly (arylene ether ketone sulfone)s functionalized with diethylenetriamine-modified graphene oxide as proton exchange membranes for fuel cells. *Int. J. Hydrogen Energy* **2024**, *73*, 609–618. [CrossRef]
41. Kim, J.; Hwang, S.; Jeong, Y.; Choi, Y.-S.; Kim, K. Cross-Linked Sulfonated Poly(arylene ether sulfone) Membrane Using Polymeric Cross-Linkers for Polymer Electrolyte Membrane Fuel Cell Applications. *Membranes* **2023**, *13*, 7. [CrossRef] [PubMed]
42. Zhao, Z.; Liu, D.; Zhong, J.; Li, J.; Lin, Z.; Zhao, Z.; Pang, J. Poly(aryl ether sulfone ketone) with densely sulfonated structural units facilitate microphase separation to promote proton transport. *J. Membr. Sci.* **2024**, *693*, 122319.